

Pluriannual Watershed Discharges of Hg into a Tropical Semi-Arid Estuary of the Jaguaribe River, NE Brazil

Luiz D. Lacerda,^{a,*} Francisco J. S. Dias,^a Rozane V. Marins,^a Talita M. Soares,^a
José Marcos O. Godoy^b and Maria Luiza D. P. Godoy^c

^aLaboratório de Biogeoquímica Costeira, Instituto de Ciências do Mar,
Universidade Federal do Ceará, Av. Abolição, 3207, 60.165-081 Fortaleza-CE, Brazil

^bDepartamento de Química, Pontifícia Universidade Católica, 22.453-900 Rio de Janeiro-RJ, Brazil

^cInstituto de Radioproteção e Dosimetria (IRD-CNEN), CP 37750, 22642-970 Rio de Janeiro-RJ, Brazil

Fluxos de Hg foram determinados entre 2005 e 2009 nas estações seca e chuvosa no estuário do Rio Jaguaribe, que desagua no Oceano Atlântico Equatorial, NE do Brasil. Na estação chuvosa a massa d'água no estuário apresenta um curto tempo de residência no estuário (0,8 dias), quatro vezes menor que na seca (3,1 dias). As concentrações e fluxos de Hg dissolvido (< 0,7 µm) e particulado foram maiores na interface rio/estuário que na estuário/mar, acumulando Hg particulado na região estuarina. A exportação de Hg particulado (1,8 a 12,6 mg s⁻¹) ao oceano ocorreu sob chuva extrema, enquanto a exportação de Hg dissolvido foi quase zero na estação chuvosa e de até 0,45 mg s⁻¹ na seca. Como a lixiviação continental no semiárido é afetada por mudanças climáticas globais e dos usos da terra, um aumento da acumulação de Hg particulado nos estuários e uma maior exportação de Hg dissolvido para o oceano é esperada.

Mercury fluxes were measured during the dry and rainy seasons (2005 to 2009) at the Jaguaribe River estuary, which discharges into the Equatorial Atlantic Ocean in NE Brazil. During rainy periods, the water masses exhibited a short residence time within the estuary (0.8 days). During dry periods, seawater choked the fluvial discharge, resulting in longer residence times (3.1 days). Dissolved (< 0.7 µm) and particulate Hg concentrations and fluxes were greater from the river to the estuary than from the estuary to the sea, producing accumulated particulate Hg in the estuary. Particulate Hg export (1.8 to 12.6 mg s⁻¹) to the ocean occurred during extremely rainy periods, while dissolved Hg export was practically nonexistent during rainy periods and increased up to 0.45 mg s⁻¹ during dry periods. Because continental runoff in semi-arid regions is affected by land use and global climate changes, the increasing accumulation of particulate Hg in the estuaries and increasing export of dissolved Hg to the ocean are expected.

Keywords: mercury, partitioning, continental discharge, hydrochemistry, hydrodynamics

Introduction

Meso- and macro-tidal estuaries with semi-arid climates tend to accumulate sediments of fluvial origin, which may be washed out to the ocean during short but intensive rain periods.¹ Where freshwater discharge is artificially controlled by river damming to provide water for human uses, as in the case of the semi-arid northeastern region of Brazil, the intensity of the rainy season runoff is further reduced, and the deposition of sediments in estuaries increases, enlarging river beaches and forming new islands

and inland deltas that are rapidly colonized by mangroves.² Under such a scenario, particle-reactive pollutants may accumulate to relatively high concentrations, even in areas where significant anthropogenic sources are absent. In the absence of intense rainy season runoff, the water residence time in the estuary may increase due to the larger tidal volume within the estuary, resulting in longer water residence times and consequently augmenting the reactivity of pollutants that may generate dissolved species prior to exportation to the sea.^{3,4} These two mechanisms can further escalate the exposure of the aquatic biota to water-borne pollutants and eventually affect the human populations that are dependent on natural resources, particularly fisheries.

*e-mail: ldrude@fortalnet.com.br

The continental flux to the ocean is extremely difficult to estimate due to the varying residence time of fluvial waters induced by the strong seasonality of semi-arid rivers, as materials originating in the continental shelf can be imported to estuaries during the long dry season. In the case of dammed rivers, the exportation of continental materials can also depend on dam operation rather than on the natural variation of the fluvial flux.⁴ To properly assess continental fluxes to the ocean, studies covering longer period of time are required, in particular in regions highly sensitive to climate and land use changes, such as in the semiarid coast of northeastern Brazil.

Mercury, a global class pollutant, appears to be especially affected by this variable hydrodynamic scenario, which has resulted in poor estimates of Hg continental flux from semi-arid regions to the ocean. Suspended particles extensively remove Hg from the water column in choked coastal areas, leading to accumulation in bottom sediments.⁵⁻⁷ The remaining dissolved Hg fraction may interact with dissolved organic matter and other complexing species, increasing the concentration of Hg dissolved species and, consequently, its mobility and bioavailability.^{8,9} Additionally, part of the Hg deposited in bottom sediments can be mobilized back to surface waters through interstitial water migration, which is mostly associated with dissolved organic carbon and also results from methylation processes within the sedimentary environment.^{10,11}

In the Jaguaribe Estuary, located in the semi-arid region of NE Brazil, Hg emissions reach approximately 250 kg yr⁻¹ and are largely from anthropogenic sources, in particular from inadequate solid waste disposal (150 kg yr⁻¹) and wastewater discharge (75 kg yr⁻¹).¹² The fraction of this input that is eventually exported to the continental shelf is unknown and is difficult to estimate due to the extreme variability of the fluvial flow induced by semi-arid conditions and reservoir operation. In the Jaguaribe River, Hg that reaches the fluvial systems is mostly associated with particles and is therefore expected to follow the same transport pathways as suspended sediments (i.e., being trapped in the estuarine environment).⁷ However, the enhanced interactions between dissolved and particulate species due to the higher residence times of the fluvial water mass during the long dry season may result in altered chemical partitioning in the water column.

In this study, we present an estimate of the Hg mass balance in the Jaguaribe Estuary based on pluriannual analyses and simultaneous determinations of river fluxes at the river-estuary and estuary-sea interfaces, which were used to estimate Hg export to the continental shelf off of the Jaguaribe coast and understand its variability and response to hydrodynamics. We used stable isotopes (¹⁸O

and deuterium ratios) to establish the mixing of water masses throughout the estuary during the dry and rain seasons. Because northeastern Brazil is one of the areas most affected by global climate change, a discussion of Hg behavior under this scenario is also presented.

Study site

The Jaguaribe basin covers approximately 72,000 km², representing almost half of Ceará State's territory in northeastern Brazil. The uniqueness of this basin is being totally enclosed into the semi-arid domain, with an average annual rainfall increasing from 400 mm inland to approximately 1,000 mm at the coast. Sandy coastal plains with large aeolian dune fields, driven by the nearly year-round constant winds from the SE, characterize the coastline. The Jaguaribe river mouth harbors an estuarine zone located between 4°23'26''S and 4°36'58''S, 37°43'58''W and 37°43'45''W (Figure 1). Its brackish tidal flood plains are covered by approximately 13,000 ha of mangroves.²

The regional climate, including rainfall seasonal variations, is regulated by the Inter-Tropical Convergence Zone (ITCZ), where air masses from both hemispheres converge. During the austral winter and spring, the ITCZ weakens and moves northward, resulting in very dry months with strong eastern winds in the Southern hemisphere. The magnitude of the ITCZ displacement is affected by El Niño teleconnections and can intensify aridity and modify the coastal geomorphology (e.g., sand dune features) that dominates Ceará's coastline. The local semi-arid climate of the lower Jaguaribe Basin displays an average annual rainfall increasing from 730 mm at Itaiçaba (35 km inland, with an average wind speed of 6.3 to 7.9 m s⁻¹) to 980 mm at Aracati (17 km from the mouth). The historical rainfall data indicate two characteristic periods, one with higher precipitation, up to 700 mm, with peak precipitation (200 to 400 mm) occurring between March and April, and a dry period with lower rainfall, typically less than 300 mm and with 1 to 3 months interval, frequently between August and November, when no precipitation is observed.²

The tidal regime is predominantly semi-diurnal, with a maximum amplitude reaching 2.8 m. The generally low freshwater supply results in the intrusion of high salinity water a few km inland. The Jaguaribe River was responsible for approximately 70% of the total occidental Northeastern Brazilian coast's freshwater input to the adjacent Atlantic Ocean prior to the building of major dams and increasing water withdraw for urbanization, agriculture and aquaculture. The average historical (past 40 years) annual freshwater discharge varied from 60 to

$130 \text{ m}^3 \text{ s}^{-1}$. However, with the building of the newest dam at the Castanhão Reservoir in 2003 ($7.9 \times 10^9 \text{ m}^3$ of storage capacity), the annual freshwater input to the ocean decreased further to approximately $20 \text{ m}^3 \text{ s}^{-1}$. In addition, the actual water discharges to the ocean, as well as the material fluxes, are highly dependent on the estuarine hydrological dynamics.³

Material and methods

Site selection and sampling strategy

Since 2005, regular field campaigns were performed during the peak of the dry and rainy seasons in two transects positioned roughly at the interface between the river (mostly fluvial-dominated conditions) and the estuary (mixing zone), with 5 sampling campaigns during the 2005-2009 period, and between the estuary and the sea (mostly marine-dominated conditions), with 3 campaigns during the 2005-2009 period (Figure 1). These sections were chosen according to the variation in the estuarine mixing zone, representing the contribution of the drainage basin to the estuary, and included regions further towards the adjacent coastal zone.^{3,13} These interfaces were chosen based on their average water conditions, but they moved along the estuary depending on the intensity of rainfall or the strength of the dry season. For each campaign, the total rainfall 30 days prior to the start of the campaign was recorded.

Our sampling strategy consisted of monitoring of the hydrodynamics (instantaneous water flux, channel depth, salinity and temperature) along each transect at hourly intervals, totaling 13 measurements in each campaign and in each transect. The measurements and sample collection were performed in triplicate in the middle section of the transects at 0.5 m depth and were used to estimate the water residence time within the estuary. The hourly sampling of water for dissolved (0.25 L bottles, $n = 39$) and particulate Hg (1.5 L bottles, $n = 39$) covered complete tidal cycles in each transect. Ten campaigns, five per transect, were performed during the 2005-2009 period to monitor hydrodynamics and to estimate the water residence time in the estuary; water samples were also collected in all these campaigns.

Hydrochemistry and hydrodynamics

The estuarine channel outflows were quantified using an acoustic current meter (ADP, 1500 kHz, SONTEK/YSI) slowly trawled by a boat, and measurements were taken along the two cross sections established in the Jaguaribe River (Figure 1). Unlike conventional current meters, ADPs

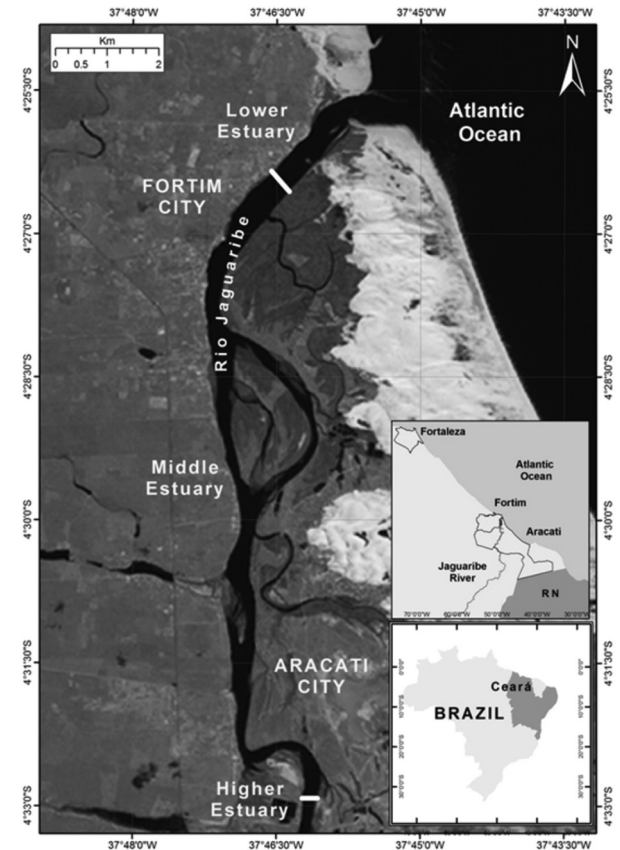


Figure 1. Location map of the Jaguaribe River estuary, NE Brazil. Cross-sections marked by a white line indicate the locations of the ADP profiles and water samplings at the river-estuary and estuary-sea interfaces.

measure current profiles by using three sound beams to determine velocity in three dimensions. Thus, ADPs measure not only the horizontal velocity, as conventional current meters do, but also the vertical component. The size of the vertical cell was 25 cm. Hourly profiles were registered for 13 hours, covering a complete tidal cycle for each cross section. The vertical and horizontal velocities were recorded every five seconds within a range of 0.1 to 1.000 cm s^{-1} , with a precision of $\pm 1\%$ for the horizontal velocity and a resolution of 0.1 cm s^{-1} .¹⁴ The CTD (conductivity, pressure and temperature) were obtained with a Sontek YSI probe. Based on the calibration, the results of the CTD data were $\pm 0.05 \text{ SU}$ and $\pm 0.02 \text{ }^\circ\text{C}$. The sampling rate of the CTD was 15 Hz.

The instantaneous discharges of the total suspended solids (TSS) and dissolved and particulate Hg were calculated according to equations 1 and 2, after Miranda *et al.*¹⁵

$$D_{spm} = \iint_A \varphi \vec{v} \cdot \vec{n} \, dA = \iint_A \varphi u \, dA = \bar{\varphi} \bar{u} A \quad (1)$$

where D_{spm} = TSS instantaneous discharges (kg s^{-1}); \bar{u} = mean velocity of the water column (m s^{-1}); $\bar{\varphi}$ = mean TSS concentration (mg L^{-1}) and A is the section area (m^2),

for each hour measured. The wet section of each profile varies in time, therefore an ADP profile was obtained for each hourly wet section.

$$D_{mi} = \int_0^{1/T} \gamma_i Q \quad (2)$$

where D_{mi} = dissolved or particulate Hg instantaneous discharges (mg s^{-1}); γ_i = dissolved or particulate Hg concentrations in water (ng L^{-1}); Q is outflow ($\text{m}^3 \text{s}^{-1}$), measured for each hour; and T is tidal period of 12.4 hours in the study area.

δ (D) and δ (^{18}O) determination

In the dry and rainy seasons of 2009, a sampling campaign in both seasons and during low tide was conducted in the river, estuary, plume and shelf waters to characterize the contribution of the different water sources to the estuarine mixing in the extreme rainfall that occurred in that year. Duplicate surface (0.5 m depth) water samples were collected in each region. Samples δ (D) and δ (^{18}O) were determined by applying ring-down cavity spectrometry using a PICARRO water isotope analyzer L1102i. Each duplicate sample was analyzed eight times. The first four results were discarded, while the last four were retained, and the observed mean values and standard deviations calculated. The measurement sequence consisted of IAEA-SMOW2 (Vienna Standard Mean Ocean Water 2), IAEA-GISP (Greenland Ice Sheet Precipitation), sample validation, six unknown samples, IAEA-SLAP2 (Standard Light Antarctic Precipitation 2), sample validation, and six unknown samples. Based on the IAEA standards' measurement results, a calibration curve was built, and the corrected delta (δ) values were calculated. The validated sample represents a water sample that was sent to six different laboratories, and the sample was subsequently used to monitor the sample results obtained from batch to batch. The typical uncertainty observed was 0.1‰ for both δ (D) and δ (^{18}O).

Mercury analysis

Careful trace-metal clean techniques were used during the sampling, storage, transport and analysis of the water samples, following the procedures of Gill and Fitzgerald.¹⁶ In summary, all glass- and plastic-ware used in the sampling and preparation of samples were decontaminated by immersion in 10% (v/v) Extran solution (MERCK), followed by immersion in diluted HNO_3 (10% v/v) for at least 2 days before a final rinse with Milli-Q water. A comparison between PET (polyethylene terephthalate),

glass and FET (Teflon fluorinated ethylene propylene) bottles showed similar and lower Hg blank values and detection limits for PET (blank = 0.09; DL = 0.18 ng L^{-1} ; $n = 9$) and FET (blank = 0.08; DL = 0.16 ng L^{-1} ; $n = 9$) but poor results from glass bottles (blank = 1.60; DL = 2.26 ng L^{-1} ; $n = 9$). Therefore, based on a cost/benefit analysis, the water samples were collected in PET plastic bottles following the protocols described by Fadini and Jardim.¹⁷

For dissolved and particulate Hg measurements, the samples were immediately filtered through quartz fiber filters (0.7 μm pore diameter). The filters were heated to 450 °C for 12 hours and transported enclosed in petri dishes prior to use. Blank concentrations from the filters reached ($0.3 \pm 0.02 \text{ ng g}^{-1}$). All chemical reagents used were of at least analytical grade. The details of the Hg analytical procedures can be found in Marins *et al.*¹⁸ In brief, the total dissolved Hg was analyzed in filtered non-acidified subsamples (50 mL) after oxidation with a bromine monochloride solution (KBrO_3 1% (m/v) + HCl 20% (v/v)) at room temperature, followed by the addition of an acidic (1% (v/v) distilled HCl + 1% (m/v) ascorbic acid) solution and reduction with 10% SnCl_2 . This fraction ($< 0.7 \mu\text{m}$) included mostly truly dissolved ionic (Hg^{2+}), plus DGM (dissolved gaseous mercury – Hg^0) and soluble colloidal Hg complexes. The samples were analyzed in duplicate, and the analytical precision, estimated as the relative percent difference between aliquots, was always less than 20%. The recovery of known additions of Hg^{2+} to filtered estuarine waters averaged $92 \pm 4\%$.

The particulate Hg concentration was calculated from the Hg quantification in the filters and TSS determination. The filters extracts were obtained by oxidation with a 50% (v/v) *aqua-regia* solution ($4\text{H}_2\text{O} : 3\text{HCl} : 1\text{HNO}_3$) at 70 to 80 °C for 1 h in Teflon vials in a MARS-Plus microwave furnace, followed by a reduction with the same SnCl_2 solution used for reducing the dissolved Hg fraction. All samples were also analyzed in duplicate. The differences between duplicates remained below 15% for all samples. For quality assurance of the Hg determination in the TSS, a certified reference material (NRC PACS-2, Canada) was simultaneously analyzed ($n = 6$), and the analysis demonstrated an average Hg recovery of $103 \pm 4\%$.

Cold vapor atomic fluorescence spectrophotometry (PSA Millennium Merlin 10.025 equipment) was used for Hg determination. The Hg detection limit, estimated as three times the standard deviation of reagent blanks, was 0.30 ng g^{-1} in suspended matter and 0.18 ng L^{-1} in water. In all cases, the blank signals were lower than 0.5% of sample analysis. The concentration values were not corrected for the relative recoveries obtained for the certified material.

For statistical analysis, the non-detectable concentrations were set as equal to half the detection limit of the method.

Results

Hydrodynamics

The extreme dry and rainy seasons in 2009 encompass all flux possibilities which occurred between 2005 and 2009, with the largest rainfall difference 330 mm and 8 mm between the rainy and the dry season, respectively. The behavior of water fluxes during the tidal cycles in the Jaguaribe River estuary in the extreme rain and dry seasons of 2009 is exemplified in Figure 2. For all other sampling periods, water fluxes behavior is somewhat between the extremes observed in 2009.

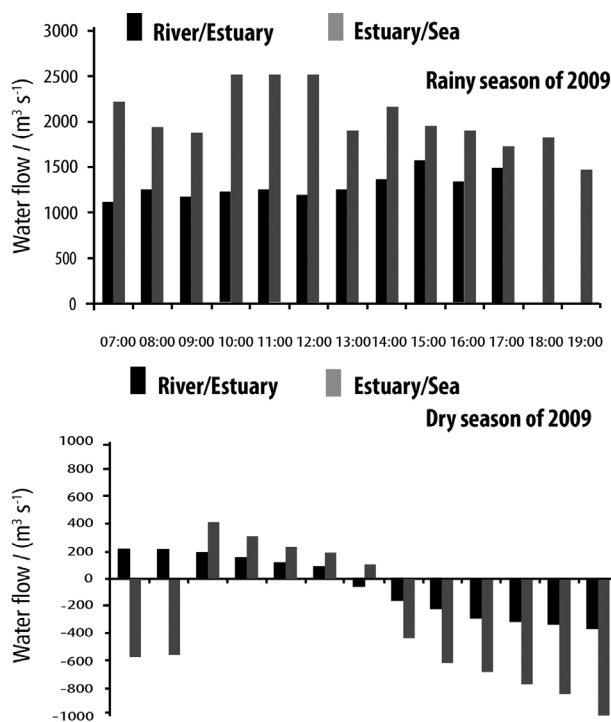


Figure 2. Typical water fluxes from river to estuary and from estuary to sea during tidal cycles in the Jaguaribe River estuary during the rainy and dry seasons of 2009. Note the permanent positive water flux to the ocean in the rain season, while during the dry season flow's direction change with tide.

During the rainy season, a positive net flux to the ocean occurred. However, even during the extreme rainy period of 2009, the marine waters contributed significantly to the total flow, mostly from the estuary to the sea, as can be observed by the much larger flow at this interface, compared to from the fluvial to the estuary. During the dry season, discharge to the ocean was mostly due to tidal waters entering the estuary, with a small contribution from the higher basin.

Between 2005 and 2009, as a result of differences in the water flow, the water residence time in the middle estuary varied significantly between seasons (Figure 3). Shorter residence times of less than one day were typical of the rainy periods, when freshwater fluxes were maximal and mostly positive, as in 2009. During the rainy seasons, the proportion of fresh water to the total estuarine volume present in the middle estuary ranged from 70% in low precipitation rainy seasons to 95% in the extreme rainy season of 2009, resulting in water residence times in the estuary that varied from 0.5 in high-rainfall rainy seasons to a maximum of 3 days in low-rainfall rainy seasons (average 0.8 days for the rainy seasons between 2005 and 2009). In contrast, the water residence times during the dry seasons were much longer, varying from 0.2 to 13 days (average 3.1 days for the entire monitoring period) (Figure 3).

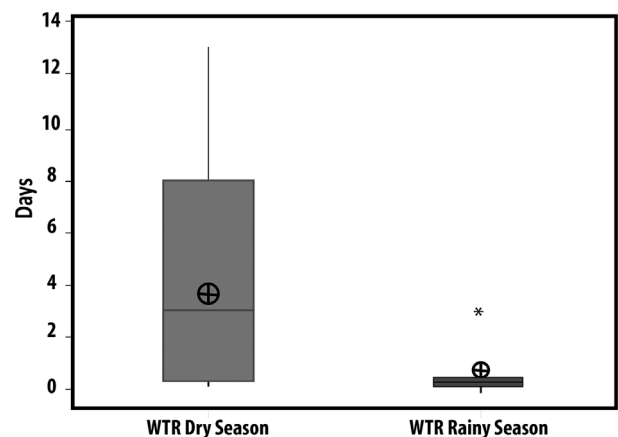


Figure 3. Water residence times (WTR) in the estuary of the Jaguaribe River during the dry and rainy seasons. The average values were derived from ADP measurements ($n = 13$) taken annually between 2004 and 2009 along the Jaguaribe River Estuary.

Figure 4a shows a typical δ (D) versus δ (^{18}O) plot observed in the extreme rainy season in 2009. The plot involves two end-members, sea water (higher δ values) and the river water (lower δ values), and a straight line connecting them, representing the mixing region. Due to surface water evaporation, this line has a smaller slope than does the Local Meteoric Water Line (LMWL).²⁰ As a consequence of the local high temperatures and semi-arid climate, the LMWL already exhibits a smaller slope than does the Global Meteoric Water Line (GMWL). The results also suggest that the Jaguaribe River water dominated the estuarine region, and even part of the plume, in this extreme season, which is in agreement with the estimated small water residence time in the estuary. In addition, some samples considered to be shelf water was, in reality, a mixture with fresh water. One apparent outlier involving a shelf water sample was observed; this may represent the

existence of an additional contribution to the water mass in this region, at least during this period of the year. As previously reported elsewhere,²¹ a good linear regression was observed between $\delta(D)$ or $\delta(^{18}O)$ and salinity, with a higher coefficient of determination for $\delta(D)$ ($r^2 = 0.902$) than for $\delta(^{18}O)$ ($r^2 = 0.841$).

A completely reversed situation was observed during the dry season. All samples indicated the strong influence of the shelf water. Additionally, the situation of a mixture of two end-members was not precisely followed, with a deviation observed at the upper-right side of the figure (Figure 4b). This finding may suggest the presence of additional water sources, in particular a submarine groundwater discharge (SGD) originating from the large sand dune fields in this region. This source is represented by the sample labeled as river water, with high positive $\delta(D)$ and $\delta(^{18}O)$. This SGD could also help to explain why the estuarine and the plume samples presented with higher δ values than the shelf samples did. An additional explanation for this observed deviation may involve the increased residence times of the waters in the estuary during the dry season, which increases the evaporation of the retained water and leads to heavier water that is clearly observed with the river samples at the Aracati transect (river/estuary interface), with a greater influence of the waters trapped inside the mangrove area that dominates the middle estuary. The Fortim (estuary/sea interface) transect samples already represent the estuarine region and, therefore, exhibit the same signature as some plume samples. No correlation of the δ values with the salinity was observed during the dry season, mainly due to the scattering of the δ values at high salinity.

Figure 5 shows the data from both sampling campaigns; the $\delta(D)$ versus $\delta(^{18}O)$ presents a deviation from the Global Meteoric Water Line (GMWL) with a slope of 6.1 and a negative deuterium excess parameter of 1.0. This value was likely due to seawater-atmospheric water vapor interactions and the non-equilibrium isotopic fractionation of groundwater after its infiltration and underground circulation.²² According to Meredith *et al.*²³ a slope lower than that of the GMWL is a trend that is often observed in arid to semi-arid environments where rainfall can undergo evaporation as it falls to the ground through dry air. In summary, the isotopic composition of water masses confirms the differences in water residence time in the estuarine region between the rainy and dry seasons.

Distribution of Hg concentrations

Tables 1 and 2 show salinity, TSS and Hg concentrations in water collected at both interfaces at the Jaguaribe River; river to estuary and estuary to sea, respectively, during the

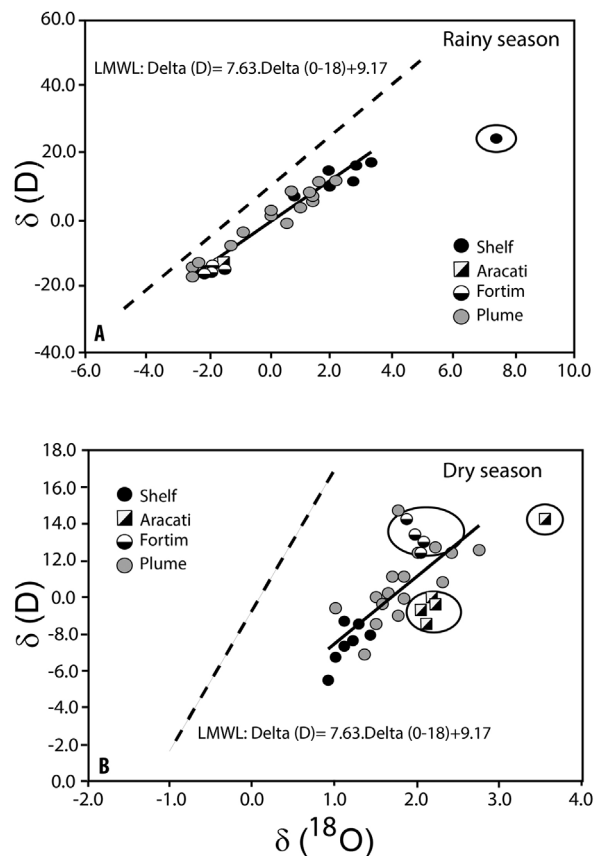


Figure 4. Isotope ($\delta(D)$ and $\delta(^{18}O)$) along the river-ocean gradient at the Jaguaribe River in the rain and dry seasons (solid lines) of 2009 compared to the Local Meteoric Water Line (LMWL) (dotted lines).

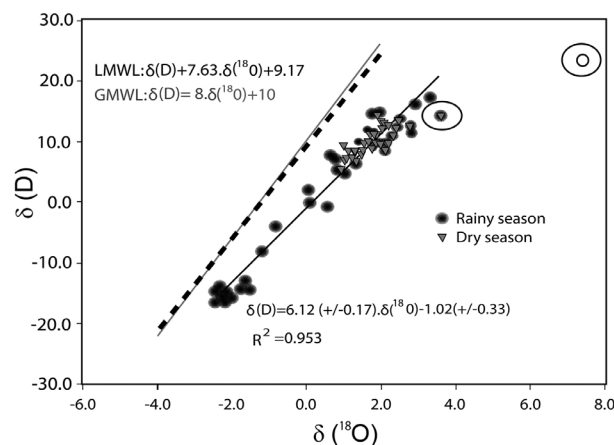


Figure 5. $\delta(D)$ versus $\delta(^{18}O)$ data from both sampling campaigns (solid black line) and their deviation from the Global Meteoric Water Line (GMWL) (solid gray line) and the Local Meteoric Water Line (LMWL) (dotted line).

monitored period. The salinity distribution indicated that the marine waters affected the entire estuary during the dry periods, both during ebb and flood tides in the river-to-estuary interface (8.4 to 26.5) and from the estuary to the sea (17.7 to 35.3). During the rainy season, the salinity values characterize fluvial waters dominating the entire

Table 1. Hydrology, total suspended sediments (TSS) and the concentrations of Hg in the TSS, particulate (Hg-P) and dissolved (Hg-D) fractions mercury in the waters, at the river/estuary interface in the Jaguaribe River, Northeastern Brazil

September 2005 dry season 30-day precipitation before sampling (mm) = 0						
Variable	Ebb			Flood		
	Minimum	Maximum	Average	Minimum	Maximum	Average
Tide / m	2.1	3.1	2.5	2.5	3.3	3.0
Salinity	24.8	27.9	26.5	24.7	30.9	28.0
TSS / (mg L ⁻¹)	10.3	34.0	15.6	7.0	11.4	9.6
Hg-TSS / (ng g ⁻¹)	159	720	361	154	700	342
Hg-P / (ng L ⁻¹)	1.6	24.5	5.6	1.1	8.0	3.3
Hg-D / (ng L ⁻¹)	1.2	44.0	15.4	< 0.18	10.2	3.9
June 2006 wet season 30-day precipitation before sampling (mm) = 70						
Variable	Ebb			Flood		
	Minimum	Maximum	Average	Minimum	Maximum	Average
Tide / m	1.1	2.2	1.6	1.3	2.5	1.9
Salinity	1.2	1.8	1.5	1.2	1.8	1.4
TSS / (mg L ⁻¹)	22.4	44.8	35.3	23.4	35.7	28.7
Hg-TSS / (ng g ⁻¹)	73	162	110	102	152	128
Hg-P / (ng L ⁻¹)	1.7	7.3	3.8	2.4	5.4	3.7
Hg-D / (ng L ⁻¹)	< 0.18	1.4	0.7	< 0.18	3.3	1.7
February 2008 wet season 30-day precipitation before sampling (mm) = 25						
Variable	Ebb			Flood		
	Minimum	Maximum	Average	Minimum	Maximum	Average
Tide / m	0.3	2.7	1.4	0.9	3.5	2.05
Salinity	18.9	26.6	22.7	24.9	32.5	29.4
TSS / (mg L ⁻¹)	5.2	10.8	7.8	6.4	12.4	9.5
Hg-TSS / (ng g ⁻¹)	86.1	174.3	129.8	80.7	113.0	95.2
Hg-P / (ng L ⁻¹)	0.4	1.9	1.0	0.5	1.4	0.9
Hg-D / (ng L ⁻¹)	< 0.18	< 0.18	< 0.18	< 0.18	< 0.18	< 0.18
May 2009 wet season 30-day precipitation before sampling (mm) = 330						
Variable	Ebb			Flood		
	Minimum	Maximum	Average	Minimum	Maximum	Average
Tide / m	0.04	0.18	0.07	0.07	0.33	0.20
Salinity	0.1	0.1	0.1	0.1	0.1	0.1
TSS / (mg L ⁻¹)	66.8	75.4	71.5	71.6	75.2	73.6
Hg-TSS / (ng g ⁻¹)	15.5	24.5	19.8	15.9	22.4	19.1
Hg-P / (ng L ⁻¹)	1.0	1.8	1.4	1.1	1.7	1.5
Hg-D / (ng L ⁻¹)	< 0.18	< 0.18	< 0.18	0.18	11.9	6.7
November 2009 dry season 30-day precipitation before sampling (mm) = 8						
Variable	Ebb			Flood		
	Minimum	Maximum	Average	Minimum	Maximum	Average
Tide / m	0.2	2.1	1.1	0.3	2.2	1.4
Salinity	4.0	12.8	8.4	2.7	17.0	9.4
TSS / (mg L ⁻¹)	18.7	19.8	19.3	11.8	20.6	17.5
Hg-TSS / (ng g ⁻¹)	4.5	21.6	13.1	13.2	15.5	14.3
Hg-P / (ng L ⁻¹)	0.08	0.4	0.3	0.2	0.3	0.3
Hg-D / (ng L ⁻¹)	2.1	6.7	4.4	1.2	4.1	2.7

estuary from the river to the sea (0.1 to 1.5). The TSS concentrations were somewhat greater during ebb and flood tides at the higher to middle estuary interface, suggesting a net contribution of continental material. At the middle to the lower estuary interface, however, the TSS concentrations were higher during flood tides, suggesting the resuspension of the deposited material, as reported previously.¹³ The maximum TSS concentrations were measured along the entire estuary in the extreme rainy season in May 2009 (65.9 to 73.6 mg L⁻¹). The Hg content in suspended particles was higher at the river-to-estuary interface in the dry periods, irrespective of tidal condition. The concentrations were also slightly increased during ebb (19.3-361 ng g⁻¹) periods, compared to flood periods (14.3-342 ng g⁻¹), at this interface, suggesting that Hg-enriched particles are entering into the estuary from the Jaguaribe basin. At the estuary-to-sea interface, however, the Hg concentrations in the TSS showed no consistent difference between ebb and flood periods but were much lower (7.8 to 93.0 ng g⁻¹) than at the river-to-estuary interface. The lower Hg content present in suspended particles at the estuary-to-sea interface and its similarity between dry and rainy periods suggests a

dominance of Hg-poor marine-born suspended particles in this region and that most Hg-rich fluvial-born suspended particles were mostly trapped within the estuary.

The particulate Hg content showed similar values, irrespective of season, between tides (ebb = 0.3-5.6 ng L⁻¹; flood = 0.3-3.7 ng L⁻¹) at the river-to-estuary interface, but these values were slightly higher than those measured at the estuary-to-sea interface, also suggesting the deposition of Hg-enriched particles and/or the release of Hg from particles as soluble species.

The dissolved Hg concentrations exhibited a completely different distribution, as compared to particulate Hg or the Hg concentrations in the TSS. During rainy periods, the dissolved Hg concentrations were lower and frequently below the detection limit of the employed methodology (< 0.2-1.7 ng L⁻¹), whereas, during dry periods, dissolved Hg could reach values higher than in the particulate fraction, as during the extreme dry period of 2005 when the dissolved Hg concentration reached an average of 15.4 ng L⁻¹. At the river-to-estuary interface, dissolved Hg concentrations did not demonstrate any trend between ebb and flood tides. At the estuary-to-sea interface, dissolved Hg was only detected

Table 2. Hydrology, total suspended sediments (TSS) and the concentrations of Hg in the TSS, particulate (Hg-P) and dissolved (Hg-D) fractions mercury in the waters, at the estuary/sea interface in the Jaguaribe River, Northeastern Brazil

February 2008 wet season 30-day precipitation before sampling (mm) = 25						
	Ebb			Flood		
	Minimum	Maximum	Average	Minimum	Maximum	Average
Tide / m	0.6	3.4	2.4	0.4	3.2	1.8
Salinity	33.6	37.0	35.1	32.7	37.5	35.3
TSS / (mg L ⁻¹)	9.3	15.4	12.6	8.8	14.8	11.6
Hg-TSS / (ng g ⁻¹)	33.1	47.5	39.4	42.8	56.6	49.8
Hg-P / (ng L ⁻¹)	0.3	0.7	0.5	0.4	0.8	0.6
Hg-D / (ng L ⁻¹)	< 0.18	< 0.18	< 0.18	< 0.18	< 0.18	< 0.18
May 2009 wet season 30-day precipitation before sampling (mm) = 330						
	Ebb			Flood		
	Minimum	Maximum	Average	Minimum	Maximum	Average
Tide / m	0.04	0.18	0.07	0.07	0.33	0.20
Salinity	0.1	0.2	0.2	0.1	0.2	0.2
TSS / (mg L ⁻¹)	54.8	77.0	65.9	62.2	81.4	72.8
Hg-TSS / (ng g ⁻¹)	91.1	94.9	93.0	22.8	77.8	48.9
Hg-P / (ng L ⁻¹)	5.0	7.3	6.2	1.4	6.3	3.6
Hg-D / (ng L ⁻¹)	< 0.18	< 0.18	< 0.18	< 0.18	< 0.18	< 0.18
November 2009 dry season 30-day precipitation before sampling (mm) = 8						
	Ebb			Flood		
	Minimum	Maximum	Average	Minimum	Maximum	Average
Tide / m	0.1	1.6	0.8	0.1	1.7	1.0
Salinity	15.3	20.1	17.7	30.6	35.0	32.5
TSS / (mg L ⁻¹)	15.2	20.7	18.0	52.8	58.2	54.8
Hg-TSS / (ng g ⁻¹)	11.4	11.7	11.5	9.0	6.6	7.8
Hg-P / (ng L ⁻¹)	0.2	0.3	0.2	0.5	0.4	0.4
Hg-D / (ng L ⁻¹)	2.1	2.3	2.2	1.7	4.6	2.9

in the dry season of 2009 and was slightly higher in the flood tide. When all detectable dissolved and particulate Hg concentrations were used to calculate an average K_d , the resulting value was $3.58 \times 10^4 \text{ kg L}^{-1}$, while most K_d values reported in estuarine areas generally range between 10^5 to 10^6 .^{6,7,24} This finding indicates that the dissolved fraction is likely overestimated due to the presence of soluble organic Hg colloids that could pass through the $0.7 \mu\text{m}$ pore size filter used in this study.

The total Hg concentrations in waters of the Jaguaribe river estuary fell within the range reported for non-contaminated estuaries,^{7,9,25-27} coastal waters^{28,29} and ocean waters.³⁰ The large variation observed in the Jaguaribe region likely reflects the strong seasonal gradients, similar to the wide range of concentrations reported for the Mackenzie River Delta in the Canadian Arctic, which is also characterized by strong seasonal variability.²⁶ As expected, the concentrations in the Jaguaribe Estuary are well below than those reported for contaminated sites.^{6,7,31-33}

Variability of the Hg fluxes

The observed instantaneous water fluxes (Table 3 and 4) were typical of a semi-arid estuary. Most of the time, the water fluxes were negative, indicating the import of marine water into the estuary and of estuarine water into the river, with ebb fluxes being trapped within the estuary inundating extensive flood plains, which are locally covered by mangroves. This pattern was only broken during the extreme rainy season of 2009, when a positive flux of fresh water (salinity < 0.2) was exported from the river to the estuary ($1,269 \text{ m}^3 \text{ s}^{-1}$) and from the estuary to the sea ($2,032 \text{ m}^3 \text{ s}^{-1}$) (Figure 2). However, even during this extreme rainy season, the water flow from the estuary to the sea was greater than that from the river to the estuary, highlighting the importance of the tidal prism.

The behavior of suspended sediment instantaneous fluxes is entirely influenced by hydrodynamics. Considering that at both interfaces there was a net accumulation of

Table 3. Water, (TSS) and particulate (Hg-P) and dissolved (Hg-D) mercury fluxes from the river to the estuary at the Jaguaribe River, Northeastern Brazil (+ = outflow; – inflow)

September 2005	Ebb			Flood			Balance ^a
	Minimum	Maximum	Average	Minimum	Maximum	Average	
Water flows / ($\text{m}^3 \text{ s}^{-1}$)	27	112	66	76	227	137	-71
TSS / (kg s^{-1})	0.27	3.80	1.02	0.53	2.59	1.31	-0.3
Flux Hg-P / (mg s^{-1})	0.04	2.74	0.37	0.08	1.82	0.45	-0.1
Flux Hg-D / (mg s^{-1})	0.03	4.92	1.01	< 0.01	2.31	0.54	+0.5
June 2006	Ebb			Flood			Balance ^a
	Minimum	Maximum	Average	Minimum	Maximum	Average	
Water flows / ($\text{m}^3 \text{ s}^{-1}$)	2	201	129	151	351	258	-129
TSS / (kg s^{-1})	0.04	9.00	4.55	3.53	12.53	7.42	-2.9
Flux Hg-P / (mg s^{-1})	0.2	32.5	14.1	15.5	53.2	33.1	-19
Flux Hg-D / (mg s^{-1})	< 0.01	0.29	0.09	< 0.01	1.15	0.45	-0.4
February 2008	Ebb			Flood			Balance ^a
	Minimum	Maximum	Average	Minimum	Maximum	Average	
Water flows / ($\text{m}^3 \text{ s}^{-1}$)	114	337	219	297	454	376	-157
TSS / (kg s^{-1})	0.59	3.64	1.70	1.89	5.65	3.56	-1.9
Flux Hg-P / (mg s^{-1})	9.8	58.8	28.5	23.9	51.3	35.8	-7.3
Flux Hg-D / (mg s^{-1})	< 0.01	< 0.01	< 0.01	< 0.01	< 0.01	< 0.01	< 0.01
May 2009	Ebb			Flood ^b			Balance ^a
	Minimum	Maximum	Average	Minimum	Maximum	Average	
Water flows / ($\text{m}^3 \text{ s}^{-1}$)	1,108	1,653	1,269	-	-	-	+1,269
TSS / (kg s^{-1})	83	99	92	-	-	-	+92
Flux Hg-P / (mg s^{-1})	1.1	2.9	1.8	-	-	-	+1.8
Flux Hg-D / (mg s^{-1})	< 0.01	< 0.01	< 0.01	-	-	-	< 0.01
November 2009	Ebb			Flood			Balance ^a
	Minimum	Maximum	Average	Minimum	Maximum	Average	
Water flows / ($\text{m}^3 \text{ s}^{-1}$)	74.2	207.0	153.1	60.0	360.0	246.9	-93.8
TSS / (kg s^{-1})	0.28	0.41	0.34	0.12	0.72	0.40	-0.06
Flux Hg-P / (mg s^{-1})	0.01	0.08	0.05	0.01	0.11	0.07	-0.02
Flux Hg-D / (mg s^{-1})	0.43	0.99	0.71	0.25	0.80	0.54	-0.17

^aValues rounded to one decimal; ^bin May 2009, the flood flux was zero at this interface.

Table 4. Water, (TSS) and particulate (Hg-P) and dissolved (Hg-D) mercury fluxes from the estuary to the sea at the Jaguaribe River, Northeastern Brazil (+ = outflow; - inflow)

February 2008	Ebb			Flood			Balance ^a
	Minimum	Maximum	Average	Minimum	Maximum	Average	
Water flows / (m ³ s ⁻¹)	345	1,030	745	1,124	1,395	1,216	-471
TSS / (kg s ⁻¹)	3.20	15.91	9.37	9.93	20.65	14.15	-4.8
Flux Hg-P / (mg s ⁻¹)	0.11	0.76	0.37	0.42	1.17	0.70	-0.3
Flux Hg-D / (mg s ⁻¹)	< 0.01	< 0.01	< 0.01	< 0.01	< 0.01	< 0.01	< 0.01
May 2009	Ebb			Flood ^b			Balance ^a
	Minimum	Maximum	Average	Minimum	Maximum	Average	
Water flows / (m ³ s ⁻¹)	1,467	2,053	2,032	-	-	-	+2,032
TSS / (kg s ⁻¹)	110	170	140	-	-	-	+140
Flux Hg-P / (mg s ⁻¹)	7.2	14.9	12.6	-	-	-	+12.6
Flux Hg-D / (mg s ⁻¹)	< 0.01	< 0.01	< 0.01	< 0.01	< 0.01	< 0.01	< 0.01
November 2009	Ebb			Flood			Balance ^a
	Minimum	Maximum	Average	Minimum	Maximum	Average	
Water flows / (m ³ s ⁻¹)	109	445	276	558	998	718	-442
TSS / (kg s ⁻¹)	1.7	6.3	4.0	31	53	41	-37
Flux Hg-P / (mg s ⁻¹)	0.02	0.13	0.06	0.28	0.40	0.28	-0.22
Flux Hg-D / (mg s ⁻¹)	0.23	0.71	0.47	0.01	0.05	0.02	+0.45

^aValues rounded to one decimal; ^bin May 2009, the flood flux was zero at this interface.

sediments within the estuary, with instantaneous export rates at the river-to-estuary interface varying from -0.06 to -2.9 kg s⁻¹ and at the estuary-to-sea interface of -4.6 to -37 kg s⁻¹, thus resulting in net instantaneous accumulation rates through the entire period, which varied from 4.54 to 34.1 kg s⁻¹. The only exception to this pattern was, again, the extreme rainy season of 2009, when sediments

were exported from the river to the estuary at a rate of $+92$ kg s⁻¹, and then to the sea at a rate of $+140$ kg s⁻¹, resulting in a net instantaneous export of previously deposited estuarine sediments to the sea at $+48$ kg s⁻¹.

On a long term basis, this continuous trapping of sediments within the estuary has been linked to the erosion of the river mouth, buildup of estuarine islands and enlargement of fluvial beaches.^{2,33} Marins *et al.*³⁴ also reported high sediment accretion rates of 0.31 cm yr⁻¹ in the Jaguaribe estuary. These observations suggest that, even considering the large instantaneous export of sediments during extreme rainfall events, a net deposition scenario dominates the Jaguaribe estuary in the long term.

The particulate Hg fluxes demonstrated instantaneous export rates at the river-to-estuary interface ranging from -0.02 to -19 mg s⁻¹ and at the estuary-to-sea interface of -0.22 to -0.30 mg s⁻¹. Therefore, over the entire period, the net instantaneous fluxes varied from an accumulation of 0.20 mg s⁻¹ of particulate Hg to a net export flux upriver

of 18.7 mg s⁻¹. During the extreme rainfall season of 2009, the particulate Hg behavior was similar to that of TSS, with instantaneous export fluxes from river to estuary of $+1.8$ mg s⁻¹ and from estuary to sea of $+12.6$ mg s⁻¹. These balances suggest a shifting export and retention of particulate Hg upstream of the estuary (Figure 6A and 6B) most of the year, but they show a net exportation of particulate Hg to the sea during extreme rain events. Notably, during the 2009 rainy season, the maximum income to the estuary was 1.8 mg s⁻¹ (Figure 6A and Table 3), but the outflow from the estuary to the sea reached 12.6 mg s⁻¹ (Figure 6B and Table 4). This finding suggests the resuspension of particles enriched with Hg to the water column when passing through the estuary.

Dissolved Hg fluxes could only be detected in 3 campaigns at the river-to-estuary interface and only in one campaign at the estuary-to-sea interface (Tables 3 and 4, respectively). In February 2008 and May 2009, the dissolved Hg concentrations were below the detection limits of the methods used, therefore hampering the estimation of the dissolved Hg fluxes. The instantaneous transport rates varied from an export from river to estuary of $+0.5$ mg s⁻¹ to an estuary to river export of -0.17 to -0.4 mg s⁻¹. Over the entire measurement period, a small net export upstream of approximately 0.07 mg s⁻¹ occurred mostly during the dry periods of 2005 and 2009. Only during

the dry season of 2009 were dissolved Hg concentrations higher than the detection limits at the estuary-to-sea interface. In this season, a net export of $+0.45 \text{ mg s}^{-1}$ was observed. The buildup of dissolved Hg throughout the estuary characterizes the Jaguaribe River estuary as a net exporter of dissolved Hg to the sea, in particular during the dry season (Figures 6C and 6D). However, the low number of detectable fluxes of dissolved Hg measured in the Jaguaribe estuary renders this hypothesis preliminary (given the current data), notwithstanding the large amount of measurable concentrations detected in individual water samples during the dry season. Previous results obtained by estimating the tidal fluxes of different Hg species from the mangrove tidal creeks^{7,10,35} strongly suggest that the flooded mangroves export dissolved, reactive Hg to the adjacent coastal waters.

Discussion

The results for the hydrodynamics of the Jaguaribe River estuary have clearly drawn a scenario typical of semi-arid climates, where waters are blocked for longer periods from fluxing to the sea during the dry season (Figure 3). During the rainy season, short but intense positive fluxes occur following extreme rainfall events. The longer water residence time in the dry season favor intra-estuary reactions of continental- and marine-born materials brought in by fluvial and tidal flows. The suspended matter and Hg species fates in the Jaguaribe estuary are strongly influenced by this hydrological setting.

The variability of the Hg concentrations and partitioning during the different tidal cycles suggests that the estuary is a major exporter of particulate Hg during the short, but sometimes intense, rainy period. During the dry season and when the rainy season is characterized by less intense rainfall, the estuary traps particulate Hg and even exports significant amounts upstream to the fluvial reaches. Of importance to note is that the export of dissolved Hg occurs mostly during the dry periods, both from the estuary to the sea and from the estuary to the fluvial sector. Flooded mangrove swamps have been suggested as exporters of reactive Hg to coastal waters.³⁵ Bergamaschi *et al.*²⁹ for example, estimated that the Hg yields from mangrove swamps are up to 5 times higher than values reported for typical wetlands, typifying mangroves as significant exporters of tidally driven Hg to nearby coastal areas.

When inside the estuary, dissolved Hg is likely generated by biogeochemical processes such as those associated with the dissimilatory sulfate reduction metabolism of mangrove sediments, which has been shown

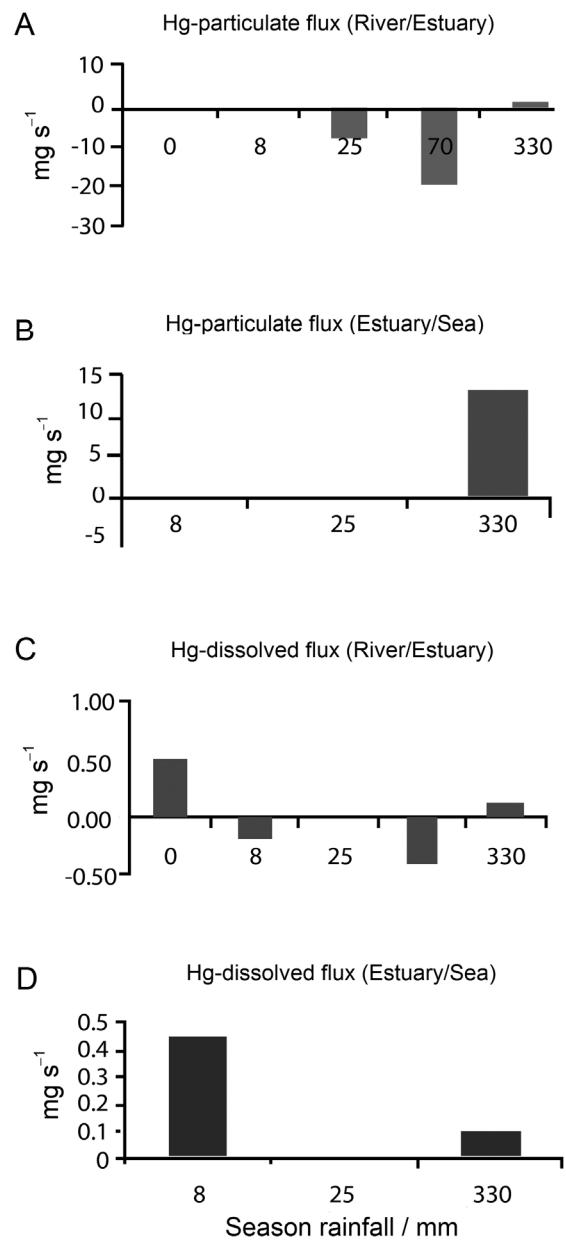


Figure 6. Dissolved and particulate Hg fluxes at the river-to-estuary and at the estuary-to-sea interfaces during different rainfall intensities at the Jaguaribe River estuary, NE Brazil. The amount of rainfall is relative to the total recorded for the 30-day period prior to each of the sampling campaigns.

to export dissolved, reactive Hg from sediments to the overlying waters, as this anaerobic metabolism results in a buildup of dissolved organic matter with a high affinity for metals.^{10,29,36} Notably, these studies found that Hg in waters exported from mangroves was more reactive with respect to methylation than was Hg in the surrounding estuarine water. The buildup of reactive Hg concentrations would be favored by the longer residence time of the water mass and the flooding of the mangrove-dominated flood plains of the Jaguaribe River during the dry season.

Assuming the average yearly flow of the Jaguaribe River to be $20 \text{ m}^3 \text{ s}^{-1}$, the total Hg flux to the sea from this river can be grossly estimated; on the average, the total annual export of Hg to the sea would reach 0.28 kg. Comparatively, the large Mackenzie River, with a water discharge of up to $30,000 \text{ m}^3 \text{ s}^{-1}$, exports a total Hg flux to the Beaufort Sea in the Arctic²⁶ of approximately 2,900 kg yr⁻¹; the Sepetiba watershed in Rio de Janeiro ($160 \text{ m}^3 \text{ s}^{-1}$) exports a total Hg flux to Sepetiba Bay of 201 kg yr⁻¹, most of which is retained inside the bay with export flux to the sea enriched with soluble Hg species, similar to the results shown in this study.⁷ The Churchill River, USA ($100\text{-}3,000 \text{ m}^3 \text{ s}^{-1}$), exports to Hudson Bay $37 \pm 28 \text{ kg yr}^{-1}$,³⁷ whereas the Siberian rivers, Lena, Ob and Yenisei, with average total annual water discharges varying from 429 to $620 \text{ m}^3 \text{ s}^{-1}$, export a total Hg load to the Arctic Ocean of 700 to 4,000 kg yr⁻¹.³⁸ The very small contribution of the Jaguaribe River is in accordance with the semi-arid conditions of this part of the Brazilian coast but may also suggest the high accumulation capacity of the estuary, decreasing the net Hg export the sea.

Implications of climate variation in the Jaguaribe estuary: the arctic paradox

The hydrodynamics of the Jaguaribe River estuary is dependent on the regional climate and regional land use changes. The Northeastern Brazilian coast is one that is most affected by global climate changes, and their effects on fluvial flows, which are already greatly altered by damming, are already significant. For example, Godoy and Lacerda³⁹ reported a 5.6 mm yr^{-1} decrease in annual rainfall over the region from the late 1960s, confirming previous results from modeling exercises by the IPCC.⁴⁰ The resulting progressive decrease in basin runoff was further accelerated by the construction of 5 dams of large size ($> 10^9 \text{ km}^3$ water storage capacity) and over 80 small to medium size reservoirs along the Jaguaribe basin in the past 50 years.^{3,13,34} The impacts of global climate change on Hg export to the sea from the semi-arid NE region of Brazil may find a parallel with the changes presently occurring in rivers draining into the Arctic Ocean, another region of Earth extremely affected by global change.^{41,42} In the Arctic, many recent studies have shown that increased continental runoff and breakage of the ice cover in estuaries resulted in increasing export of Hg to the Arctic Ocean,^{26,37,43} leading to higher incorporation by the phytoplankton, higher deposition in shelf sediments and increasing concentrations in the Arctic biota.^{44,45} In contrast, in the semi-arid region of Brazil, global climate changes decrease the freshwater contribution to the estuarine region and eventually the continental runoff to the sea and, therefore, should have resulted in

decreased Hg export to the sea. Paradoxically, however, similar to the Arctic, high Hg concentrations in fish from the northeastern continental shelf off the Jaguaribe River have also been reported, as well as concomitant increases in Hg and organic matter in sediment profiles.⁴⁶ As has been demonstrated here, reducing continental runoff results in an augmentation of the residence time of waters in the estuary, flooding of marginal plains dominated by mangroves and slack water conditions. During these periods, larger Hg mobilization was simultaneously observed and, in at least one occasion, resulted in higher export of dissolved and more bioavailable Hg to the sea.

Conclusion

Based on a few observations, one could expect larger Hg mobilization when the water residence time in the estuary increases, and this may occur more frequently as the continental runoff decreases. If this “Arctic Paradox” holds true, the scenario is most likely growing worse, as global climate changes will continue to reduce continental runoff in the semi-arid NE region of Brazil, and human water uses will also expand. Therefore, Hg reactivity could possibly increase in the estuary even further and when eventually exported to the adjacent coastal sea by the rarer freshwater flux peaks. These described mechanisms will increase Hg bioavailability to coastal food webs, similarly to, but paradoxically with, the situation that is presently occurring and is also expected to worsen in the Arctic.

Acknowledgements

This study is part of the INCT-TMCOcean (www.inct-tmcocean.com.br): “Continent-Ocean Materials Transfer” project supported by CNPq, Brazil, process No. 573.601/2008-9. The authors also thank the Blue Amazon Program from CAPES for providing grants to FJSD. We extend our deep thanks to the crew of the NOc Prof Martins Filho who made part of this work possible. We would like to thank Prof Edmo Campos and Rogerio Parentoni for discussing our view of the “Arctic Paradox,” as well as our many students who spent many of their weekends performing field work during these past 5 years.

References

1. Salomons, W.; Forstner, U.; *J. Soils Sediments* **2010**, 8, 239.
2. Maia, L. P.; Lacerda, L. D.; Monteiro, L. H. U.; Souza, G. M.; *Atlas dos Manguezais do Nordeste do Brasil: Avaliação das Áreas de Manguezais dos Estados do Piauí, Ceará, Rio Grande do Norte, Paraíba e Pernambuco*. SEMACE: Fortaleza, 2006.

3. Dias, F. J. S.; Lacerda, L. D.; Marins, R. V.; de Paula, F. C. F.; *Hydrol. Processes* **2011**, 25, 2188.
4. Lacerda, L. D.; Marins, R. V.; Dias, F. J. S.; Soares, T. C. M. S.; *Rev. Virtual Quím.* **2012**, 4, 456.
5. Coquery, M.; Cossa, D.; Sanjuan, J.; *Mar. Chem.* **1997**, 58, 213.
6. Lacerda, L. D.; Gonçalves, G. O.; *Mar. Chem.* **2001**, 76, 47.
7. Paraquetti, H. H. M.; Ayres, G. A.; Molisani, M. M.; Lacerda, L. D.; *Water Res.* **2004**, 38, 1439.
8. Carrie, J.; Wang, F.; Sanei, H.; Macdonald, R. W.; Outridge, P. M.; Stern, G. A.; *Environ. Sci. Technol.* **2010**, 44, 316.
9. Han, S.; Gill, G. A.; Lehman, R. D.; Choe, K.-Y.; *Mar. Chem.* **2006**, 98, 156.
10. Mounier S.; Lacerda, L. D.; Marins, R. V.; Benaim, J.; *Bull. Environ. Contam. Toxicol.* **2001**, 67, 519.
11. Fitzgerald, W. F.; Lamborg, C. H.; Hammerschmidt, C. R.; *Chem. Rev.* **2007**, 107, 641.
12. Lacerda, L. D.; Soares, T. M.; Costa, B. G. B.; Godoy, M. D. P.; *Bull. Environ. Contam. Toxicol.* **2011**, 87, 657.
13. Dias, F. J. S.; Marins, R. V.; Maia, L. P.; *Acta Limnol. Bras.* **2009**, 21, 377.
14. Polonichko, V.; Mullison, J.; Cabrera, R.; *Sea Technology* **2000**, 1, 76.
15. Miranda, L. B.; Bergamo, A. L.; Castro, B. M.; *Ocean Dynam.* **2005**, 55, 430.
16. Gill, G. A.; Fitzgerald, W. F.; *Deep-Sea Res.* **1985**, 32, 287.
17. Fadini, P. S.; Jardim, W. F.; *Analyst* **2000**, 125, 549.
18. Marins, R. V.; Paraquetti, H. H.; Ayres, G. A.; *Quím. Nova* **2002**, 25, 372.
19. Hastenrath, S.; Greischar, L.; *J. Geophys. Res.* **1993**, 98, 5093.
20. Godoy, J. M.; Godoy, M. L. D. P.; Neto, A.; *J. Geochem. Explor.* **2012**, 119/120, 1.
21. Ingham, B. L.; Conrad, M. E.; Ingle, J. C.; *Geochim. Cosmochim. Acta* **1996**, 60, 455.
22. Povinec, P. P.; Oliveira, J.; Braga, E. S.; Comanducci, J. F.; Gastaud, J.; Groening, M.; Levy-Palomo, I.; Morgenstern, U.; *Top. Z.; Estuarine, Coastal Shelf Sci.* **2008**, 76, 522.
23. Meredith, K. T.; Hollins, S. E.; Hughes, C. E.; Cendón, D. I.; Hankin, S.; Stone, D. J. M.; *J. Hydrol.* **2009**, 378, 313.
24. Turner A.; Milward, G. E.; Le Roux, S. M.; *Environ. Sci. Technol.* **2001**, 35, 4648.
25. Turner, A.; *Mar. Chem.* **1996**, 54, 27.
26. Leitch, D. R.; Carrie, J.; Lean, D.; Macdonald, R. W.; Stern, G. A.; Wang, F.; *Sci. Total Environ.* **2007**, 373, 178.
27. Sarica, J.; Amyot, M.; Hare, L.; *Water, Air, Soil Pollut.* **2004**, 151, 3.
28. Ci, Z.; Zhang, X.; Wang, Z.; Niu, Z.; *Mar. Chem.* **2011**, 126, 250.
29. Bergamaschi, B. A.; Krabbenhoft, D. P.; Aiken, G. R.; Patino, E.; Rumbold, D. G.; Orem, W. H.; *Environ. Sci. Technol.* **2012**, 46, 1371.
30. Mason, R. P.; Sullivan, K. A.; *Deep-Sea Res.* **1999**, 46, 937.
31. Balcom, P. H.; Hammerschmidt, C. R.; Fitzgerald, W. F.; Lamborg, C. H.; O'Connor, J. S.; *Mar. Chem.* **2008**, 109, 1.
32. Covelli, S.; Acquavita, A.; Piani, R.; Predonzani, S.; De Vittor, C.; *Estuarine, Coastal Shelf Sci.* **2009**, 82, 273.
33. Godoy, M. D. P.; Lacerda, L. D.; *J. Coastal Res.* **2013**, DOI 10.2112/JCOASTRES-D-13-00059.1.
34. Marins, R. V.; Paula-Filho, F. J.; Rocha, C. A. S.; *Quím. Nova* **2007**, 30, 1208.
35. Lacerda, L. D.; Silva, L. F. F.; Marins, R. V.; Mounier, S.; Paraquetti, H. H. M.; Benaim, J.; *Wetlands Ecol. Manage.* **2001**, 9, 323.
36. Jaffé, R.; Boyer, J. N.; Lu, X.; Maie, N.; Yang, C.; Seully, N. M.; Mock, S.; *Mar. Chem.* **2004**, 84, 195.
37. Kirk, J. L.; St. Louis, V. L.; *Environ. Sci. Technol.* **2009**, 43, 2254.
38. Coquery, M.; Cossa, D.; Martin, J. M.; *Water, Air, Soil Pollut.* **1995**, 80, 653.
39. Godoy, M. D. P.; Lacerda, L. D.; *Arq. Ciênc. Mar* **2013**, in press.
40. Intergovernmental Panel for Climate Change (IPCC). *Synthesis Report. Contributions of Working Groups I, II and III to the fourth assessment report of the inter-governmental panel on climate change*; IPCC: Geneva, 2007.
41. Macdonald, R. W.; Harner, T.; Fyfe, J.; *Sci. Total Environ.* **2005**, 342, 5.
42. Outridge, P. M.; Macdonald, R. W.; Wang, F.; Stern, G. A.; Dastoor, A. P.; *Environ. Chem.* **2008**, 5, 89.
43. Graydon, J. A.; Emmerton, C. A.; Lesack, L. F. W.; Kelly, E. N.; *Sci. Total Environ.* **2009**, 407, 2980.
44. Braune, B. M.; Outridge, P. M.; Fisk, A. T.; Muir, D. C. G.; Helm, P. A.; Hobbs, K.; Hoekstra, P. F.; Kuzky, Z. A.; Kwan, M.; Letcher, R. J.; Lockhart, W. L.; Norstrom, R. J.; Stern, G. A., Stirling, I.; *Sci. Total Environ.* **2005**, 351/352, 4.
45. Rigét, F.; Braune, B.; Bignet, A.; Wilson, S.; Aars, J.; Born, E.; Dam, M.; Dietz, R.; Evans, M.; Evans, T.; Gamber, M.; Gantner, N.; Green, N.; Gunnlaugsdóttir, H.; Kannan, K.; Letcher, R.; Muir, D.; Roach, P.; Sonne, C.; Stern, G.; Wiig, O.; *Sci. Total Environ.* **2011**, 409, 3520.
46. Costa, B. G. B.; Soares, T. C. M.; Torres, R. F.; Lacerda, L. D.; *Bull. Environ. Contam. Toxicol.* **2013**, 90, 537.

Submitted: May 5, 2013

Published online: September 4, 2013